Journal of Highway and Transportation Research and Development
2024, 18(4): 67−77

Research Article
ISSN 2095−6215
DOI: 10.26599/HTRD.2024.9480029

Braking control strategy of distributed electric vehicle based on vehicle velocity prediction

Meiying Li[1*], Chengxin Li[1], Xuebo Li[2], Shu Wang[1], Xuan Zhao[1]

1. *School of Automobile, Chang'an University, Xi'an, Shaanxi 710000, China*;
2. *School of Mechanical and Electrical Engineering, Xi'an University of Architecture and Technology, Xi'an, Shaanxi 710000, China*

Abstract: To enhance the efficiency of braking energy recovery in distributed electric vehicles, this study investigates the impact of vehicle velocity prediction on braking performance. A regenerative braking control strategy that incorporates vehicle velocity prediction is proposed. Initially, a vehicle velocity prediction model is developed using a back-propagation neural network, which is trained under various operational conditions, and its validity is confirmed through testing. Subsequently, a braking control strategy that integrates vehicle velocity prediction is formulated based on a parallel braking control approach to optimize braking energy recovery. Finally, simulations of the proposed control strategy are conducted and compared with a strategy that does not utilize velocity prediction, under both joint working conditions and the Worldwide Harmonized Light Vehicles Test Cycle (WLTC). The findings indicate that the control strategy utilizing vehicle velocity prediction achieves greater energy recovery in both scenarios, with improvements in braking energy recovery efficiency of 9.2% and 6.13% over the non-predictive strategy, respectively. These results demonstrate the efficacy and rationale of the proposed approach.

Keywords: automotive engineering; velocity prediction; energy recovery; control strategy

1 Introduction

Distributed electric vehicle employs four motors integrated into each wheel and controlled independently, resulting in higher braking energy recovery efficiency compared to a general centralized drive electric vehicle. This feature gives it broad application prospects[1]. However, different braking energy recovery control strategies will affect braking stability and energy recovery effectiveness. There are two common control strategies for braking energy recovery: rule-based and optimization algorithm-based. Among them, the rule-based control strategy is widely used due to its simple structure and easy implementation. On the basis of the original front-rear axle brake torque distribution ratio, Zhang et al.[2] only adjusted the front axle mechanical brake system, and proposed three control strategies: maximum energy recovery, best pedal feel and coordinated control strategy. Li et al.[3] considered the brake pedal opening, its change rate, vehicle speed, and battery state of charge (SOC) as inputs to a fuzzy controller, putting forward a regenerative braking control strategy to improve the efficiency of regenerative braking energy recovery.

It is worth noting that vehicle velocity is crucial for braking energy recovery. Having prior knowledge of the operating conditions enables parameter adjustments according to the control strategy, thereby enhancing the energy recovery effect to some extent. Several studies have focused on enhancing the precision and accuracy of vehicle velocity prediction methods. Baker et al.[4] predicted future vehicle speed by combining historical vehicle speed and longitude information. Yu et al.[5] utilized a backpropagation neural network (BPNN) to learn velocity prediction abilities over a finite horizon using standard driving cycles. Wang et al.[6] employed a generalized regression neural network (GRNN) to predict future speed and introduced an accurate prediction input sequence into a multi-objective optimization energy management strategy.

Therefore, a prediction model based on BPNN to fore-

Received: 26 December 2023; **Revised:** 13 March 2024; **Accepted:** 19 April 2024

* *E-mail address*: 313538791@qq.com

cast the vehicle velocity under joint working conditions is put forward in this study, predicted result is taken as input of fuzzy controller. Based on this, a braking energy recovery control strategy is presented, leveraging vehicle velocity prediction. The effectiveness of this strategy is validated through simulation.

2 System model

The structure of the compound braking system for distributed electric vehicles is depicted in Figure 1. Information interaction and communication between the vehicle control unit (VCU), motor, and battery units are facilitated through the Controller Area Network (CAN). When the driver initiates a braking command by pressing the brake pedal, the command is first transmitted to the VCU. Subsequently, the controller assesses the feasibility of energy recovery during braking. Frictional braking torque is generated by the mechanical braking system, while feedback braking torque is generated by the motor. These two torques are combined at the wheel to execute the vehicle braking process. Throughout this period, the motor operates in a braking state, generating power, the feedback current is then employed to charge the battery, enabling the storage of the recovered energy.

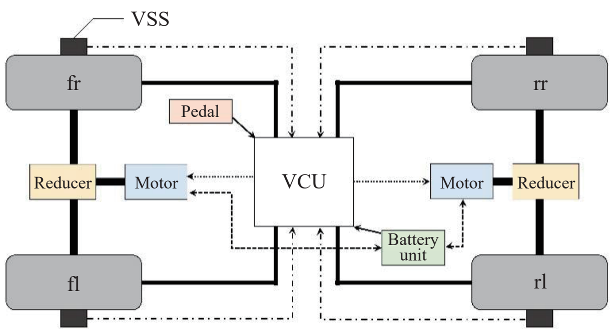

Fig. 1 Compound braking system structure of distributed electric vehicle

To conduct a comprehensive investigation into the recovery of braking energy in distributed electric vehicles, a system model is established, encompassing the vehicle's dynamic model, motor model, and battery model.

2.1 Vehicle dynamic model

The longitudinal motion of the vehicle body is only considered in this paper, there is no difference between the left and right braking torques for each wheel (front and rear)[7]. Thus, a half-vehicle model is established, as shown in Figure 2.

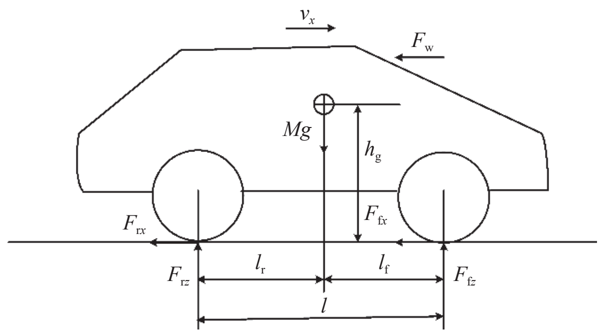

Fig. 2 Half-vehicle model

In the scenario of straight-line braking, the rolling resistance can be disregarded, allowing the longitudinal motion of the vehicle to be expressed as Equations (1) and (2):

$$M\dot{v}_x = -F_{fx} - F_{rx} - F_w, \tag{1}$$

$$F_w = C_D A_f {v_x}^2/21.15, \tag{2}$$

where, M is the vehicle mass; v_x is the longitudinal velocity; F_{fx}, F_{rx} are the front and rear wheel tire-road friction forces; F_w is the aerodynamic drag force; C_D is the aerodynamic drag coefficient; A_f is the front window windward area.

The vertical loads on the front and rear wheels can be obtained by Equations (3) and (4):

$$F_{fz} = M(l_r g - h_g \dot{v}_x)/l, \tag{3}$$

$$F_{rz} = M(l_f g + h_g \dot{v}_x)/\mathrm{l}, \tag{4}$$

where, F_{fz}, F_{rz} is the longitudinal front and rear wheel normal forces separately; g is the gravity acceleration; l is the distance between the front and rear axles; l_f and l_r are the distances from the gravity center to the front and rear wheel respectively; h_g is the height of the gravity center.

2.2 Motor model

The function of the motor is transferring the electric energy of the battery to the drive controller as well turn it into the mechanical energy required for the vehicle to drive. The permanent magnet synchronous motor (PMSM) is utilized to fulfill the power requirements of the vehicle, including maximum speed, maximum gradeability, and acceleration performance. The relationship between the braking torque and the motor speed is displayed in Figure 3, where T_m and ω_m represent the braking torque and speed of the motor, respectively.

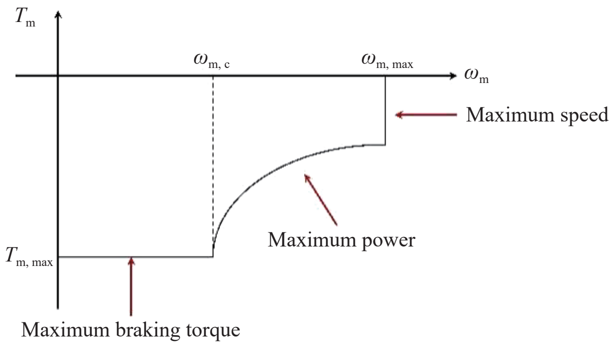

Fig. 3 Characteristic curve of motor

The figure reveals that the motor braking process is constrained by three conditions. Firstly, at low speeds, the maximum braking torque is limited to $T_{m,max}$ due to current limitations. Secondly, because of the common limitation of current and voltage, the maximum braking power is $P_{m,max}$. Lastly, the maximum speed of the motor is $\omega_{m,max}$, establishing the third constraint. The motor braking torque is described as a first-order inertia link as Equation (5):

$$T_m = T_{m,ref}/(\tau_m s + 1), \tag{5}$$

where, $T_{m,ref}$ is the reference braking torque of the motor; T_m is the actual output torque of the motor; τ_m is the inertia time constant.

2.3 Driveline model

The driveline of vehicle is crucial to the transmission of vehicle torque, which uses two main reducers, the drive shaft and other components complete the transmission of torque. The conversion between the actual braking torque and the wheel speed exerted on the wheel can be expressed as Equations (6) and (7):

$$T_{m,w} = 2\eta T_m / i_0 \tag{6}$$

$$\omega_w = \omega_m i_0 / 2\pi \tag{7}$$

where, $T_{m,w}$ is the braking torque actually acting on the wheel after passing through the reducer; ω_w and ω_m are wheel speed and motor speed; η is transmission efficiency; i_0 is reduction ratio.

2.4 Battery model

The $LiFePO_4$ battery is selected as model in this paper, which follows a basic open circuit voltage-resistance (OCV-R) formulation. The equivalent circuit consists of a voltage source and an internal resistance, both of which are function of *SOC* and battery temperature. The battery feedback power, recovered energy and *SOC* are calculated by Equations (8) to (10):

$$P_r = UI, \tag{8}$$

$$E_r = \int_0^t P_r \mathrm{d}t, \tag{9}$$

$$SOC = SOC_0 - \left(\int_0^t \eta I \mathrm{d}t\right)/C_N, \tag{10}$$

where, P_r and E_r are the feedback power and recovered energy; U and I are the battery terminal voltage and current respectively; t is the terminal moment; SOC_0 is the initial remaining battery capacity; C_N is the nominal capacity of the battery; η is charge/discharge efficiency.

In order to measure the effect of braking energy recovery, two indicators of braking energy feedback efficiency and battery *SOC* are opted separately to evaluate. The braking energy feedback efficiency can be defined as Equations (11) and (12):

$$\xi = E_r/E_0, \tag{11}$$

$$E_0 = m v_x^2/2, \tag{12}$$

where, ξ is the braking energy feedback efficiency; E_0 is the kinetic energy at the initial moment of braking. The parameters values for the system above are listed in Table 1.

3 Velocity prediction

The vehicle velocity forecast determines the vehicle state in the predicted interval, then decides the braking force distribution. This, in turn, directly impacts the braking control strategy. In this section, Back Propagation neural network is chosen as the vehicle velocity prediction model in the limited time domain in the future, the original vehicle velocity sequence is divided into training set and test set. A single neural network model is trained with the training set, the test set is used to prove the validity of the prediction method on the accuracy of the predicted vehicle velocity.

3.1 BPNN model

The Back Propagation neural network (BPNN) is a type of Artificial Neural Network (ANN) that encompasses a diverse range of architectures[8]. As shown in the Figure 4, the BPNN comprises one input layer, a number of hidden layers and one output layer. Each layer consists of a predetermined number of neurons, also referred to as nodes. The neurons within a layer are not

Table 1 System parameter values

Symbol	Property	Value
M	Vehicle mass	1 260 kg
C_D	Aerodynamic drag coefficient	0.32
A_f	Front window windward area	2.1 m^2
g	Gravity acceleration	9.8 m/s^2
l_f	Distance from the gravity center to the front wheel	1.2 m
l_r	Distance from the gravity center to the rear wheel	1.4 m
l	Distance between the front and rear axles	2.6 m
h_g	Height of the gravity center	0.54 m
$T_{m,max}$	Maximum braking torque	100 N·m
$P_{m,max}$	Maximum braking power	15 kW
$\omega_{m,max}$	Maximum speed	1 250 r/min
τ_m	Inertia time constant	0.05 s
η	Transmission efficiency	0.96
i_0	Reduction ratio	5.73
SOC_0	Initial remaining battery capacity	0.8
C_N	Nominal capacity	55 A·h

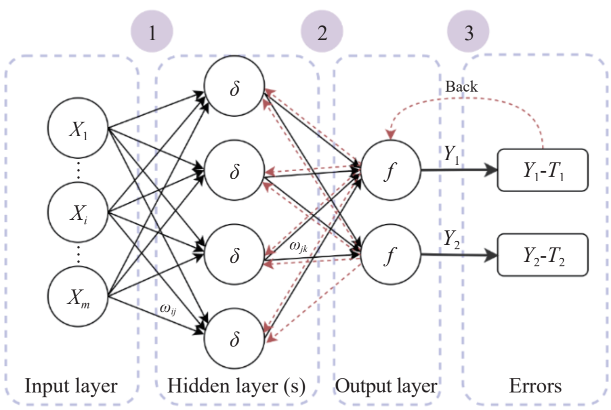

Fig. 4 Structure of BPNN

connected to one another, but connections are established between neurons with different weights across the layers.

The training process of a BPNN involves obtaining output values through the hidden layer and output layer. In this process, the deviations between the collected output values and the expected output values are calculated. The weights and thresholds are then adjusted using these deviations to continually reduce the biases and obtain more desirable outputs. The specific principles are as follows:

(1) Obtain the output of the hidden layer from the input vector, hidden layer weights, thresholds, and activation function:

$$H_j = \delta\left(\sum_{j=1}^{m} w_{ij}X_i + b_j\right). \tag{13}$$

(2) Then obtain the output of the output layer from the output of the hidden layer and the output layer weights:

$$Y_k = f\left(\sum_{i=1}^{h} w_{jk}H_j + a_k\right). \tag{14}$$

(3) Compare the obtained output with the expected result, and feedback to adjust the weight of the output layer until the error meets the requirements:

$$\Delta\omega_{ij} = \eta Y_k \sum_{k=1}^{2} (Y_k - T_k)^2/2, \tag{15}$$

$$\omega_{ij} = \omega_{ij} + \Delta\omega_{ij}, \tag{16}$$

where, $\boldsymbol{X} = (X_1, X_2, \cdots, X_m)^{\mathrm{T}}$ is the input layer contains m neurons, with the input vector; X_i is the i-th input neuron in the input layer; $\boldsymbol{Y} = (Y_1, Y_2, \cdots, Y_n)^{\mathrm{T}}$ is the output layer contains n neurons with the output vector; Y_k is the k-th output neuron in the output layer.

Each connection between an input neuron and a hidden neuron is assigned a weight ω_{ij} indicating the strength of the connection. The j-th neuron in the hidden layer has a threshold b_j that controls its activation state. The activation function of the hidden layer is denoted by δ. Each connection between a hidden neuron and an output neuron is assigned a weight ω_{jk}. The k-th neuron in the output layer has a threshold a_k, the activation function of the output layer is denoted by f, η is the learning rate, and T_k is the expected output of the k-th node.

3.2 Vehicle velocity prediction model based on BPNN

The velocity prediction in this paper uses the speed from the (k-10)th to the kth second to predict the speed of the future (k+p)th second, where p is the predicted step size. The predicted velocity is then employed as input for subsequent velocity prediction. To encompass the characteristics of speed variations in diverse driving conditions, the training data incorporates New York city cycle (NYCC), urban dynamometer driving schedule (UDDS), West Virginia University urban interstate text cycle (WVUINTER), and highway fule economy test

(HWFET). These velocity data are grouped according to the following rules:

(1) The velocity data $V_1 = (v_1, v_2, \cdots, v_t)$ serves as the first input sequence, and v_{t+1} being the expected output value.

(2) The velocity data $V_i = (v_i, v_{i+1}, \cdots, v_{t+i-1})$ serves as the i-th input sequence, and the speed data v_{t+i} is taken as the expected output value.

Once the velocity data is grouped, it undergoes normalization, and 70% of the dataset is allocated as the training set for model training. The neural network architecture employed in this study comprises a solitary hidden layer comprising 5 neurons. A learning rate of 0.05 is implemented, and upon reaching the specified threshold, the predicted output values are denormalized. The training parameters are illustrated in Table 2.

To objectively evaluate the effectiveness of the velocity prediction, Root Mean Square Error (E_{RMS}) and Mean Absolute Error (E_{MA}) are utilized as evaluation metrics, whose expressions are presented in the Table 3.

Table 2 Training parameters

Training parameters	Value
Hidden layer	1
Number of neurons	5
Learning rate	0.05
Learning threshold	0.000 001

Table 3 Evaluation index

E_{RMS}	E_{MA}
$E_{RMS} = \sqrt{\frac{1}{n}\sum_{i=1}^{n}\left(Y_i - \hat{Y}_i\right)^2}$	$E_{MA} = \frac{1}{n}\sum_{i=1}^{n}\lvert Y_i - \hat{Y}_i\rvert$

3.3 Result analysis

The correlation analysis shown in Figure 5 demonstrates that the correlation coefficients between the actual velocity and predicted velocity are almost equal to 1 for both the training set and test set. This high correlation signifies a strong relationship between the input and

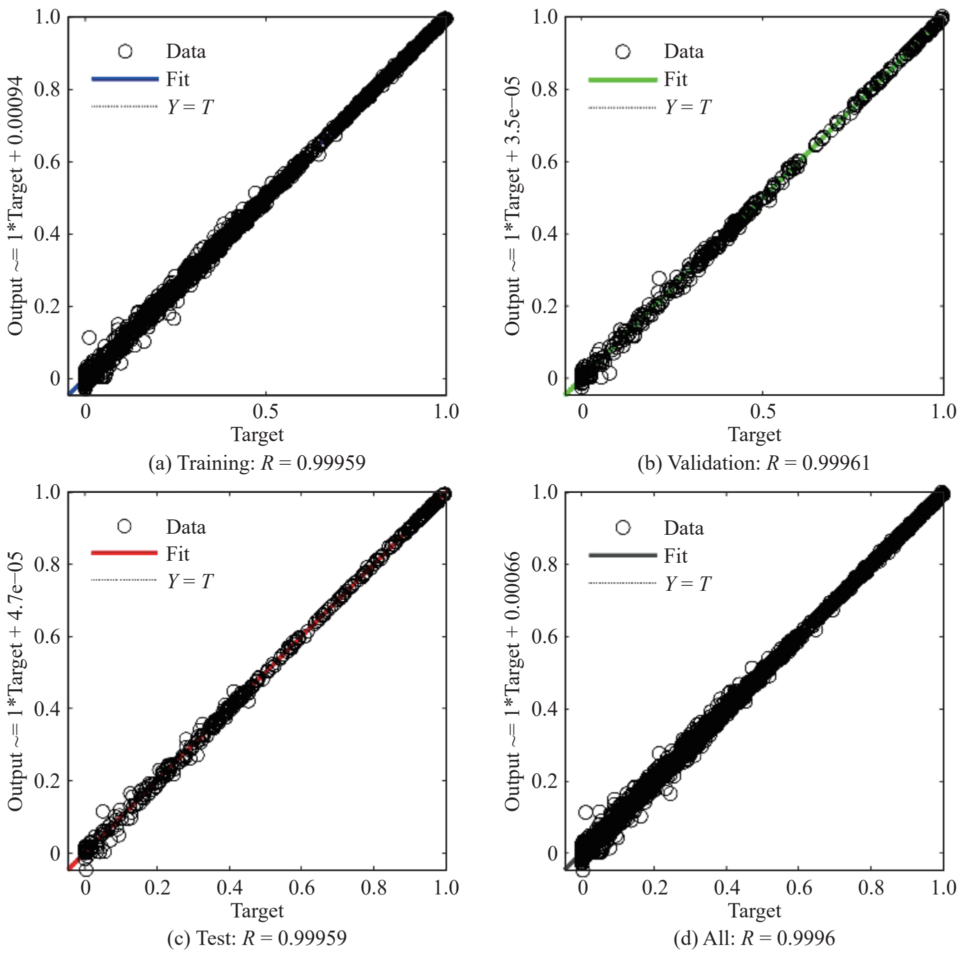

(a) Training: $R = 0.99959$ (b) Validation: $R = 0.99961$ (c) Test: $R = 0.99959$ (d) All: $R = 0.9996$

Fig. 5 Correlation analysis

output, thereby validating the trained model.

The predicted results are displayed in the Figure 6, it is evident that while there are certain inaccuracies in velocity prediction within the training set when the vehicle is stationary, overall, the training set aligns well with the training data, yielding an E_{RMS} of 0.587 3 and E_{MA} of 0.3529. Notably, the predicted velocity in the test set exhibits reduced errors compared to the expected velocity, resulting in a decreased E_{RMS} of 0.312 3 and E_{MA} of 0.1952. These findings indicate that the implemented BPNN model effectively contributes to velocity prediction, yielding favorable outcomes.

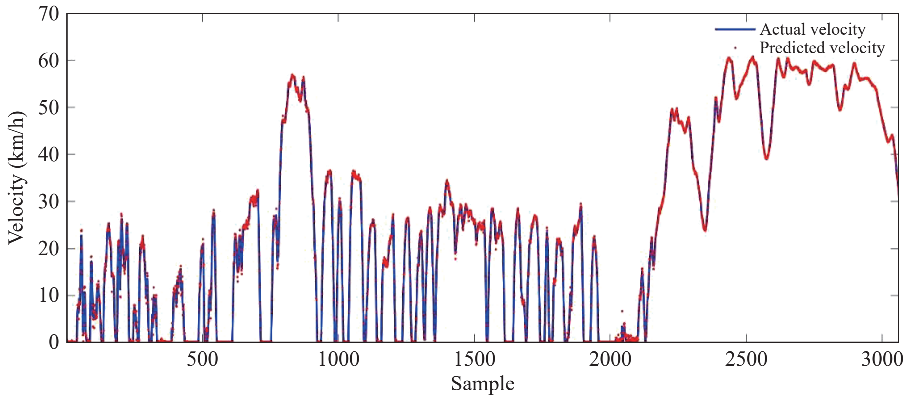

(a) Comparison of predicted and reference velocity on the training set

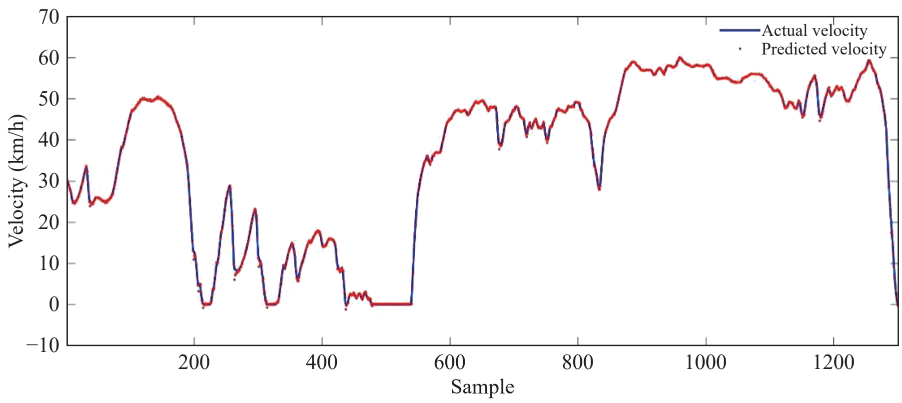

(b) Comparison of predicted and reference velocity on the test set

Fig. 6 Velocity prediction results

4 Braking control strategy

In the regenerative braking mode of electric vehicles, both the motor brake and the mechanical brake operate simultaneously. To ensure braking safety and vehicle stability, a regenerative braking control strategy is proposed. This strategy involves the coordinated distribution of motor braking and mechanical braking, along with the allocation of braking force between the front and rear axles.

4.1 Typical braking control strategy

To incorporate the braking energy recovery system into the existing braking system of electric vehicles, the braking function is achieved by reconfiguring the two braking forces. Three distinct braking control strategies are primarily employe (1) Ideal braking force distribution control strategy; (2) Optimal braking energy recovery control strategy; (3) Parallel braking energy recovery control strategy. The graphical representations of these strategies can be found in Figure 7, while a comprehensive analysis of their pros and cons is provided in Table 4.

Considering the cost and the difficulty of implementation, the parallel braking energy recovery control strategy is selected in this paper. On this basis, the fuzzy control is used and the vehicle speed prediction part is added to evaluate the efficiency of braking energy recovery.

4.2 Control strategy based on fuzzy control

The control system for electric vehicles encounters various limitations when it comes to braking energy feedback. Among these factors, the state of charge (*SOC*) of

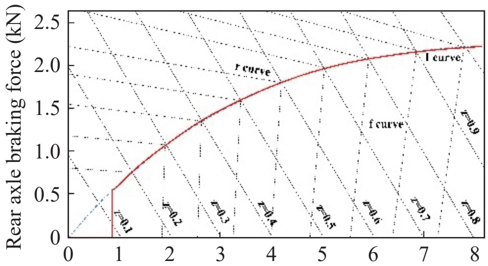

(a) Ideal braking force distribution control strategy

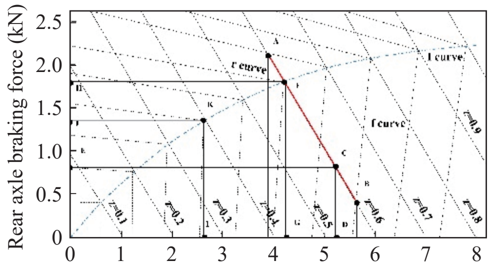

(b) Optimal braking energy recovery control strategy

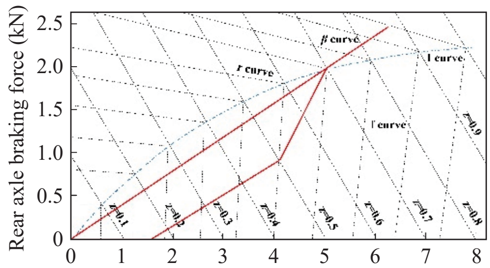

(c) Parallel braking energy recovery control strategy

Fig. 7 Braking force distribution strategy graphical representations

Table 4 Comparison of three strategies

Strategy	Pros	Cons
Ideal braking force distribution control strategy	Good braking effect and stabilityShort braking distance	Complex structure of the braking system
Optimal braking energy recovery control strategy	Recover braking energy efficiently	Complex structure of the braking system
Parallel braking energy recovery control strategy	Simple system structure	Poor regenerative braking effect

the battery, vehicle velocity (V), and braking strength (Z) have the most significant influence. Consequently, these variables are utilized as the three input parameters for the fuzzy controller. The output value, denoted as K, represents the ratio of the motor braking force to the total braking force allocated to the front axle. The primary objective is to maximize the involvement of regenerative braking force in the braking process while ensuring smooth braking, thus effectively utilizing the recycled braking energy. The system structure of designed fuzzy control strategy is illustrated in Figure 8. The driver determines the degree of brake pedal application based on the driving situation. By considering this input signal, the total braking force and braking strength of the vehicle can be determined. Building upon the parallel braking energy recovery control strategy, the allocation of regenerative braking and friction braking can be achieved.

Figure 9 illustrates the degree of membership functions for the three input parameters (V, SOC, Z) and the output value (K) in fuzzy set theory. The value of the membership function determines the extent to which each element in the domain belongs to a specific membership function. A steeper membership function indicates higher control sensitivity and resolution, while a flatter membership function contributes to better stabilization.

Under the premise of vehicle braking safety and energy recovery, a set of 27 fuzzy rules are formulated, as shown in Table 5. Each rule follows the expression: if (Z is Z_i) and (SOC is SOC_i) and (V is V_i), then (K is K_i).

5 Simulations and results

To demonstrate the effectiveness of the proposed braking energy recovery control strategy, a simulation analysis is conducted using MATLAB software. The main parameters of the vehicle are outlined in Table 1. The prediction time domain is set to 1 s, the sampling time is 1 s, and two simulation conditions are considered:

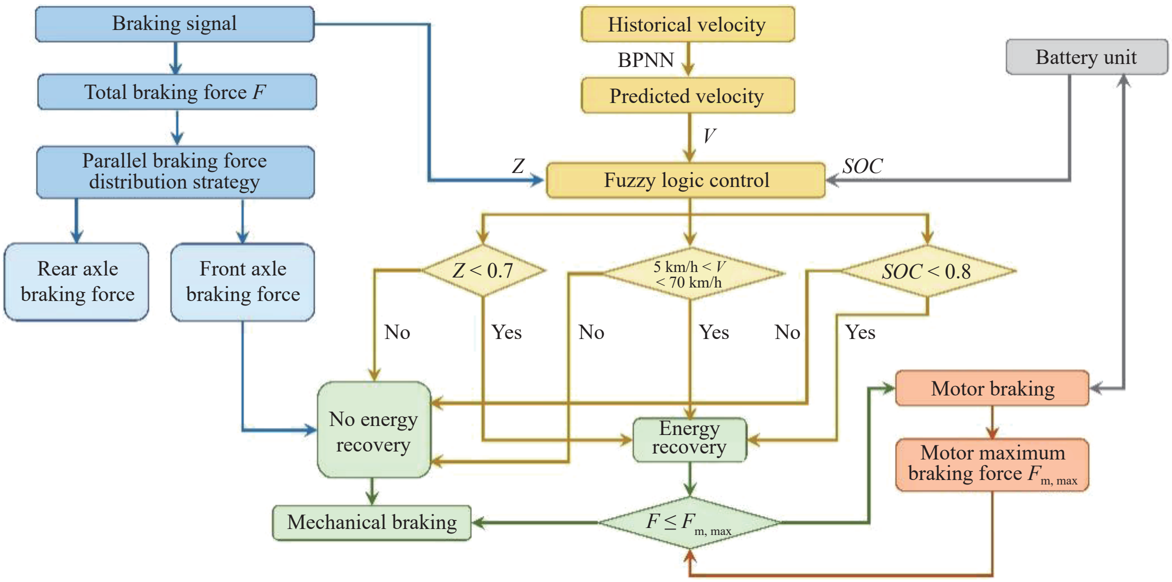

Fig. 8 System structure of fuzzy control strategy

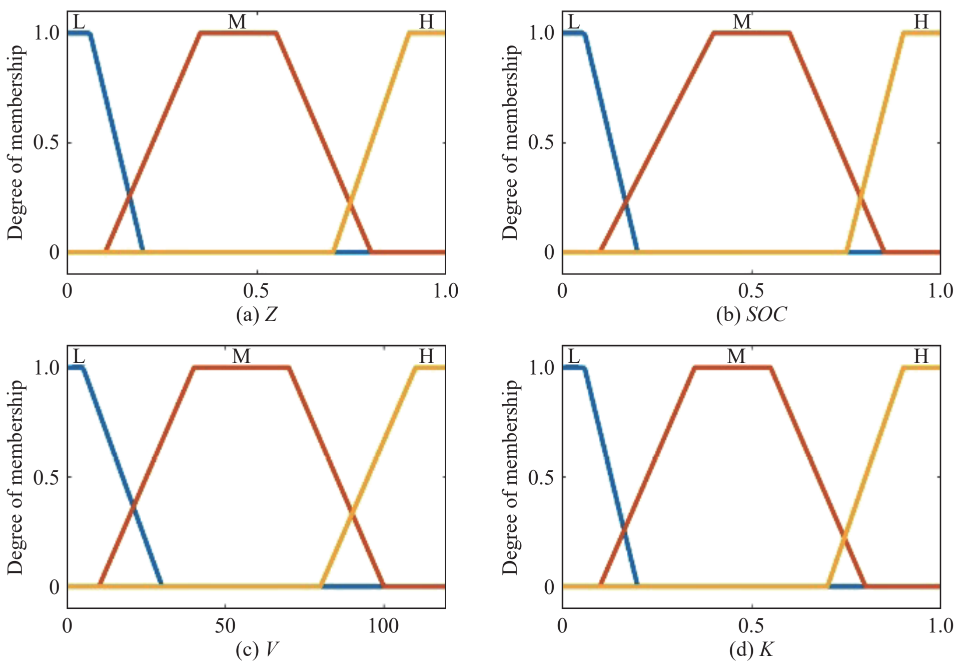

Fig. 9 Degree of membership functions

(1) Combination of NYCC, UDDS, WVUINTER and HWFET driving cycles; (2) world light vehicle test cycle (WLTC). Comparing the proposed braking energy recovery control strategy based on vehicle velocity prediction with the control strategy without vehicle velocity prediction, the simulation results are shown in the Figure 10. The E_{RMS} and E_{MA} under two conditions are listed in Table 6.

From Figure 10 and Table 6, it is evident that the proposed control strategy exhibits a favorable fitting effect under both working conditions. As the predictive model is trained using the joint working conditions, it achieves better fit in these specific cases. However, it also demonstrates applicability to other scenarios. The accuracy of the control strategy can be further evaluated by examining the *SOC* and energy recovery efficiency. The results of this evaluation are depicted in Figure 11 and summarized in Table 7.

As depicted in Figure 11, the control strategy incorporating vehicle velocity prediction exhibits reduced fluctuations in the state of charge (*SOC*) compared to the strategy without velocity prediction. Moreover, it effect-

Table 5 Fuzzy control rules

Number	*Z*	*SOC*	*V*	*K*	Number	*Z*	*SOC*	*V*	*K*	Number	*Z*	SOC	*V*	*K*
1	L	H	L	L	10	L	M	L	L	19	L	L	L	L
2	L	H	M	L	11	L	M	M	H	20	L	L	M	H
3	L	H	H	L	12	L	M	H	H	21	L	L	H	H
4	M	H	L	L	13	M	M	L	L	22	M	L	L	L
5	M	H	M	L	14	M	M	M	M	23	M	L	M	M
6	M	H	H	L	15	M	M	H	M	24	M	L	H	M
7	H	H	L	L	16	H	M	L	L	25	H	L	L	L
8	H	H	M	L	17	H	M	M	L	26	H	L	M	L
9	H	H	H	L	18	H	M	H	L	27	H	L	H	L

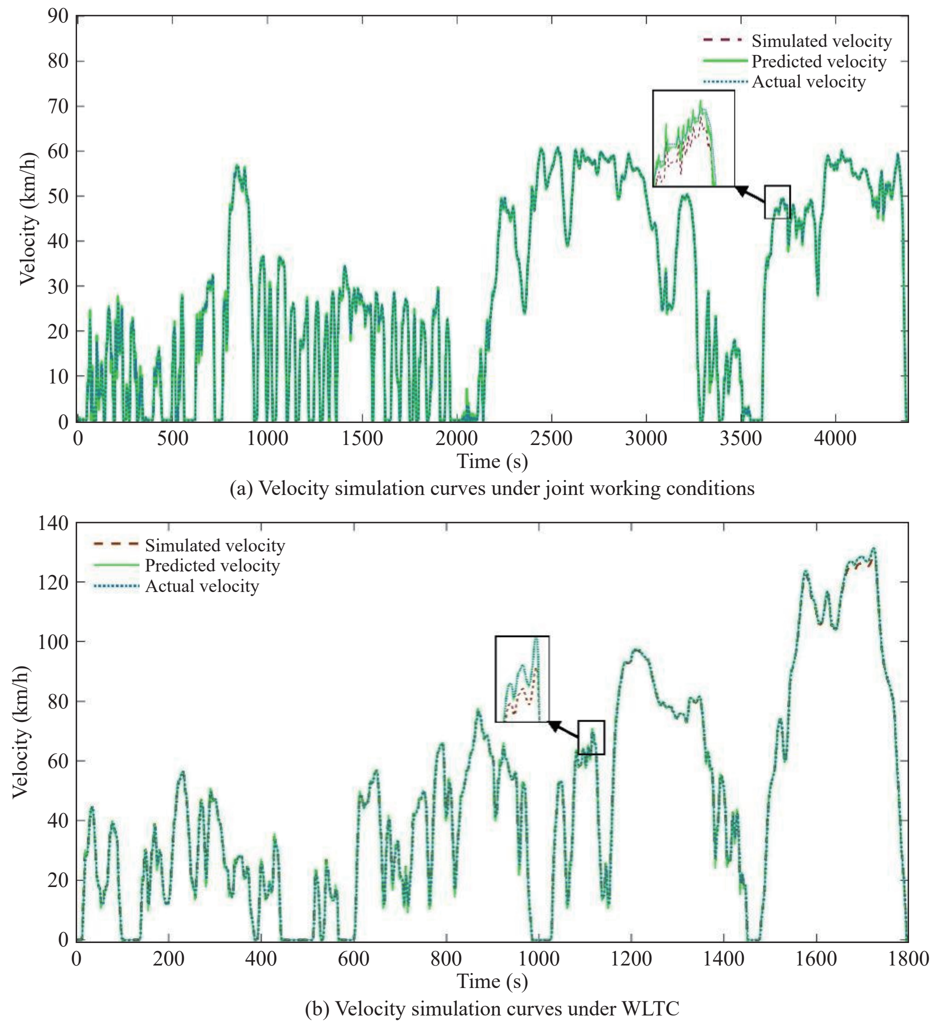

Fig. 10 Vehicle velocity simulation results

ively charges more electricity to the battery during driving. The results presented in Table 7 further reinforce this observation, highlighting that the control strategy with vehicle velocity prediction achieves higher energy recovery compared to the strategy without velocity prediction under both working conditions. Specifically, the braking energy recovery efficiency is found to be 9.2% and 6.13% higher, respectively, compared to the strategy

Table 6 E_{RMS} and E_{MA} of simulation results

Working condition	E_{RMS}	E_{MA}
Joint working conditions	0.386 9	0.229 6
WLTC	0.782 3	0.513 9

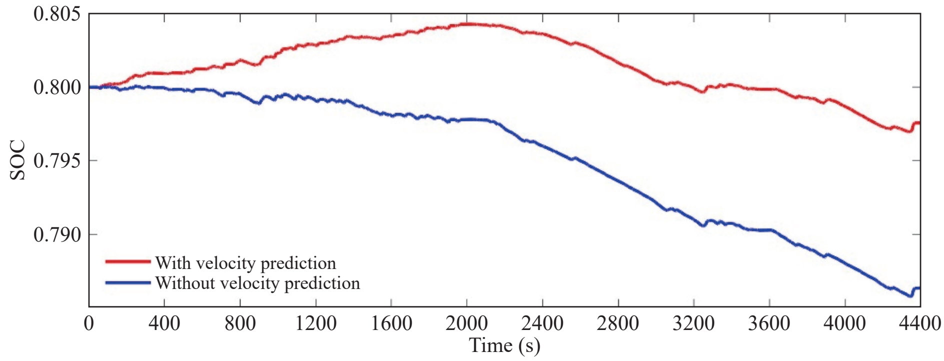

(a) SOC change curves under joint working conditions

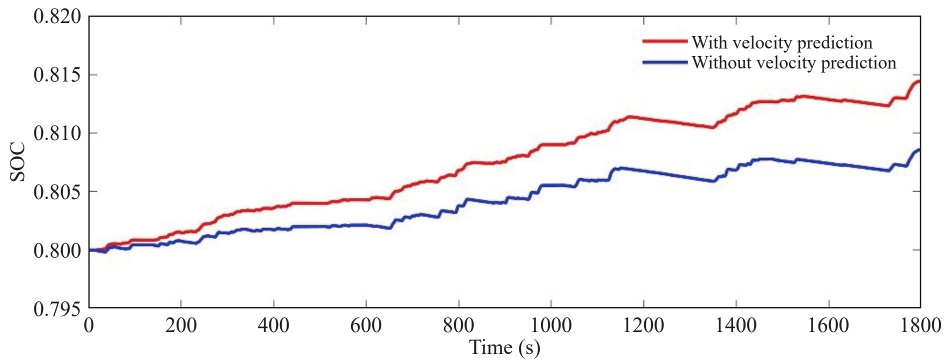

(b) SOC change curves under WLTC

Fig. 11 SOC change curves:

Table 7 Comparison of energy recovery efficiency

Working condition	Control strategy	Energy recovery efficiency (%)
Joint working conditions	With velocity prediction	76.38
	Without velocity prediction	67.16
WLTC	With velocity prediction	70.77
	Without velocity prediction	64.64

without velocity prediction.

In summary, the braking control strategy proposed in this paper, which incorporates vehicle velocity prediction, effectively ensures braking stability while achieving high efficiency in the recovery of braking energy.

6 Conclusions

In this paper, a braking control strategy that incorporates vehicle velocity prediction is proposed. The strategy is validated by training and testing a BPNN model using joint working conditions. Building upon the parallel braking energy recovery control strategy, the control strategy in this paper considers vehicle velocity information, braking strength, and *SOC* through fuzzy reasoning to determine the distribution coefficient for the front and rear axles. The feasibility of the proposed strategy is demonstrated through experiments conducted under both joint working conditions and the WLTC working condition. The results indicate that the control strategy with vehicle velocity prediction achieves higher energy recovery compared to the without one, confirming the rationality and effectiveness of the proposed strategy.

Declaration of competing interest

The authors have no competing interests to declarethat are relevant to the content of this article.

Acknowledgements

This work was supported in part by the National Natural Science Foundation of China (No. 52372375, No. 52472397); in part by the Key Research and Development Program of Shaanxi Province (2024GX-YBXM-260); in part by the Science and Technology Achievement Transformation Project of Shaanxi Province (2024CG-CGZH-19).

References

[1] Zhang, X.D., Gohlich D. A novel driving and regenerative braking regulation design based on distributed drive electric vehicles[C]//2016 IEEE Vehicle Power and Propulsion Conference (VPPC). Hangzhou: IEEE, 2016.

[2] Zhang, J.Z., Lü, C., Gou, J.F., et al. Cooperative control of regenerative braking and hydraulic braking of an electrified passenger car[J]. Proceedings of the Institution of Mechanical Engineers, Part D: Journal of Automobile Engineering, 2012, 226(10): 1289–1302.

[3] Li, C.B., Yi, Q., Hu, R., et al. Control strategy for regenerative braking based on fuzzy pattern recognition indual-motor electric vehicles[J]. Computer Integrated Manufacturing Systems, 2020, 26(4): 871–881.

[4] Baker, D., Asher, Z., Bradley, T. Investigation of vehicle speed prediction from neural network fit of real world driving data for improved engine On/Off control of the EcoCAR3 hybrid Camaro[R]. SAE Technical Paper, 2017-01-1262, 2017.

[5] Yu, S.M., Lin, D., Sun, Z., et al. Efficient model predictive control for real-time energy optimization of battery-supercapacitors in electric vehicles[J]. International Journal of Energy Research, 2020, 44(9): 7495–7506.

[6] Wang, W.D., Guo, X.H., Yang, C., et al. A multi-objective optimization energy management strategy for power split HEV based on velocity prediction[J]. Energy, 2022, 238:121714.1-121714.14.

[7] Li, W.F., Du, H.P., Li, W.H. Four-wheel electric braking system configuration with new braking torque distribution strategy for improving energy recovery efficiency[J]. IEEE Transactions on Intelligent Transportation Systems, 2020, 21(1): 87–103.

[8] Suliman, A., Yun, Z. A review on back-propagation neural networks in the application of remote sensing image classification[J]. Journal of Earth Science and Engineering, 2015, 5(1): 52–65.